

Product Isotope Effects on in Vivo Methanogenesis by *Methanobacterium thermoautotrophicum*[†]

Robin W. Spencer,[‡] Lacy Daniels,[‡] Gail Fulton, and W. H. Orme-Johnson^{*†}

ABSTRACT: The hydrogen in methane produced by cultures of *Methanobacterium thermoautotrophicum* originates from water. In H₂O/D₂O mixtures, a methane product isotope effect is observed that increases rapidly as the water deuterium enrichment approaches 100%. This effect is due to the intracellular production of protons from H₂, catalyzed by hydrogenase, which occurs at 12% the rate of water diffusion through the cell membrane. We estimate that water diffusion through the thick cell membrane of *M. thermoautotrophicum* is retarded by a factor of 10⁶ over the free diffusion rate. The

intracellular production of H⁺ suggests that either (1) hydrogenase is not directly involved in the production of a chemiosmotic proton gradient or (2) if it is involved, the proton gradient exists between the cytosol and the interior of vesicles observed in this bacterium. The intrinsic deuterium product isotope effect in methanogenesis is 1.20 ± 0.1, comparable to anabolic deuterium product isotope effects in other autotrophs. An algebraic model incorporating the intracellular H₂ to H⁺ flux accurately predicts the distribution of deuterated methane species at all levels of water deuterium enrichment.

The bacterium *Methanobacterium thermoautotrophicum* is a thermophilic obligate anaerobe that derives both its energy and cell carbon from the reduction of carbon dioxide. Some 95% of its total carbon flux is devoted to energy production in the formal reaction of eq 1, the reduction of carbon dioxide



to methane by 4 equiv of hydrogen gas. We have recently shown (Daniels et al., 1980) that all four hydrogens¹ of this methane have their origin in water and not in hydrogen gas. In this paper we extend these studies by examination of the isotopic composition of methane produced by cell cultures in several H₂O/D₂O mixtures, with the aim to answer the following questions. (1) What is the solvent product isotope effect on in vivo methanogenesis? (2) Is this observed isotope effect constant over all H₂O/D₂O ratios? (3) If not, what is the origin of this variation and what is the intrinsic isotope effect? (4) Is the intrinsic isotope effect sufficiently different from known anabolic deuterium product isotope effects to permit a distinction between anabolic and catabolic CO₂ reduction pathways in this organism?

Materials and Methods

All reagents, gases, and bacterial cultures were obtained as described previously (Daniels et al., 1980). Deuterium gas (CP) was purchased from MG Scientific Gases, Somerville, NJ.

Procedures for bacterial propagation, growth, and assay have been described, as have techniques for sample preparation and analysis by high-resolution mass spectrometry (Daniels et al., 1980). Varying levels of water deuterium enrichment were made by mixing appropriate volumes of H₂O and D₂O (99.7 atom % D; Aldrich) and were measured at the end of each experiment by proton NMR. Aliquots for analysis were taken

after 4 h of incubation unless noted otherwise (Table I). Mass spectra were taken of duplicate samples with at least three scans per sample; NMR samples were taken in duplicate with five spectra per sample, comparing water protons with added dioxane.

Results and Discussion

The distribution of the deuterated methane species produced by *M. thermoautotrophicum* in several H₂O/D₂O mixtures and under both H₂/CO₂ and D₂/CO₂ atmospheres are given in Table I. The observed product isotope effects calculated from these data (Appendix 2) are also presented.

As pointed out by Daniels et al. (1980), there are at least four different ways in which a product deuterium isotope effect could be observed in methanogenesis. First, the effect may be due to real isotope discrimination in one or more of the reductive steps that fix hydrogen to the methanogenic carbon. Within this possibility are the extreme cases (a) that there are negligible isotope effects in three of the four steps and large effect in only one and (b) that all four steps have moderate, equal isotope effects. Second, there may be no isotope discrimination in the direct methanogenic pathway but rather discrimination in a parallel, obligate step that produces a hydride-transferring cofactor, such as dihydroF₄₂₀ or NADPH. Finally, in the third and fourth cases, there may not be isotope discrimination in any methanogenic step, the observed isotope effect reflecting a higher intracellular protium concentration (i.e., lower atom % D) than the extracellular water.² In the third case such a difference in enrichment between intra- and extracellular water enrichment would be caused by a significant kinetic isotope effect in the diffusion of water through the cell membrane, and in the fourth case the difference would

[†] From the Department of Biochemistry, University of Wisconsin, Madison, Wisconsin 53706. Received February 13, 1980. This work was supported by the College of Agriculture and Life Sciences, University of Wisconsin, and by National Institutes of Health Grant GM 17,170. R.W.S. is a fellow of the Helen Hay Whitney Foundation, and L.D. is supported by a National Institutes of Health postdoctoral fellowship, Fellowship No. 5-732 GM 06600-02 BBCB.

[‡] Present address: Department of Chemistry, Massachusetts Institute of Technology, Cambridge, MA 02139.

¹ "Protium" and "deuterium" and H and D are used to refer to specific isotopes of hydrogen; "hydrogen" refers to H or D regardless of molecular attachment, and "hydrogen gas" and "water" refer to H₂, HD, or D₂ and H₂O and D₂O and any mixtures thereof. DihydroF₄₂₀ is the two electron reduced form of the 8-demethyl-8-hydroxy-5-deazaflavin coenzyme in these bacteria (Eirich et al., 1978).

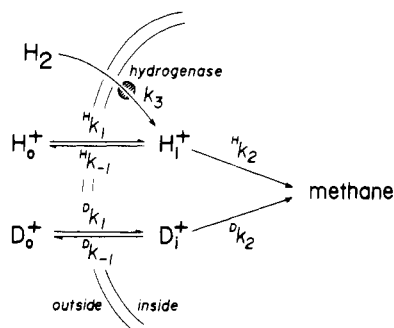
² "Intracellular" and "extracellular" are used as functional terms, recognizing that if methanogenesis takes place within enclosed vesicles within the cells (Zeikus & Wolfe, 1973; Zeikus & Bowen, 1975; Doddema et al., 1979), "intravesicular" and "extravesicular" may be more appropriate.

Table I: Distribution of Methane Species Produced at Different Water Deuterium Enrichments

water atom % D (=100 n_0)	initial atm	final hydrogen gas atom % D	methane mole fraction					methane atom % D ^a (=100 q)	obsd ^b product iso- tope effect (= α_{obsd})
			CH ₄	CH ₃ D	CH ₂ D ₂	CHD ₃	CD ₄		
±1		±2			±0.03			±2	
32.5	H ₂ /CO ₂	19	0.38	0.41	0.17	0.03	0.01	22	1.7 ± 0.2
51.7	H ₂ /CO ₂	30	0.13	0.29	0.34	0.20	0.04	42	1.5 ± 0.2
81.0	H ₂ /CO ₂	63	<0.01	0.01	0.30	0.43	0.26	74	1.5 ± 0.2
86.5	H ₂ /CO ₂	66	<0.01	<0.01	0.25	0.42	0.33	77	1.9 ± 0.2
90.4	H ₂ /CO ₂	77	<0.01	0.05	0.06	0.43	0.46	83	2.0 ± 0.3
98.7 ^c	H ₂ /CO ₂	40	<0.01	<0.01	0.08	0.36	0.56	87	11 ± 4
98.7 ^d	H ₂ /CO ₂	>48	<0.01	<0.01	0.07	0.18	0.75	92	7 ± 4
99.5 ^d	D ₂ /CO ₂	>88	<0.01	<0.01	<0.03	0.11	0.87	96	
00.0	D ₂ /CO ₂	40	0.53	0.37	0.09	0.01	<0.01	14	

^a Calculated as $q = (X_{\text{CH}_3\text{D}} + 2X_{\text{CH}_2\text{D}_2} + 3X_{\text{CHD}_3} + 4X_{\text{CD}_4})/4$. ^b Calculated as $\alpha_{\text{obsd}} = 1/q - 1/(1/n_0 - 1)$. ^c Sample taken after 2 h of incubation. ^d Samples taken after 15 h of incubation.

Scheme I



be caused by a significant internal production of H⁺ from H₂, catalyzed by one or more hydrogenases. For the latter two cases, the isotopic composition of methane can be viewed simply as a nonexchangeable probe of the H₂O/D₂O ratio of the interior of the cell. Our ability to distinguish among these possibilities in a whole cell system is discussed below for each case in turn.

If the observed isotope effect were due to approximately equal effects in each of the steps that fixes hydrogen to the methanogenic carbon (case 1b), the distribution of labeled methanes should be described by the expansion of $(p + q)^4$, where p is the probability of acquiring H at any step and q is the probability of acquiring D. If one of the steps has a much larger isotope effect than the other three (case 1a), the distribution is more complex (Appendix 1a). The methane distributions predicted in these cases differ most for large isotope effects; they naturally converge to the same simple statistical distribution as the isotope effect approaches 1. We estimate that for any observed isotope effect less than about 2, the measurement of the methane isotopic distribution by mass spectrometry is insufficiently accurate to distinguish between these cases. However, for either of these cases the observed isotope effect should be independent of the water deuterium enrichment n_0 ,³ and since this is not observed (Table I), these hypotheses can be rejected as major contributors to the observed isotope effect.

If the observed isotope effect were due to an effect only on the acquisition of hydrogen from water that is later transferred without exchange to the methanogenic carbon (case 2), the methane distribution would again be $(p + q)^4$, and the observed

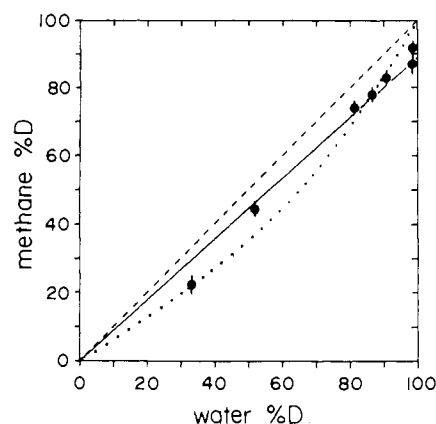


FIGURE 1: Deuterium enrichment of methane produced by *M. thermoautotrophicum* as a function of water deuterium enrichment. The initial atmosphere was H₂/CO₂ for all points. The dashed line is the expected relation ($q = n_0$) if there is neither isotope discrimination nor significant intracellular H⁺ production by hydrogenase. The dotted line is the hyperbolic relation expected if the difference in enrichment were solely due to isotope discrimination in methanogenesis and/or water diffusion through the membrane (case 3), and the solid line is the relation expected if the difference is due to intracellular production of H⁺ from H₂ catalyzed by hydrogenase (case 4).

effect would again be independent of the water enrichment. This hypothesis can thus be rejected as well.

What remains is the conclusion that apparent hydrogen isotope discrimination in methanogenesis is largely the result of different isotopic compositions of intra- and extracellular water. Cases 3 and 4 are discussed in terms of the minimal kinetic model of Scheme I and the algebra developed in Appendices 2–4. These two cases may be distinguished experimentally by examining the methane enrichment q when the hydrogen gas is changed from H₂ to D₂. The predictions of each case and the results are discussed below.

For case 3 there is no source of H⁺ or D⁺ other than the initial water, so that in 100% D₂O (under H₂ gas) the methane produced should be all CD₄ and in 100% H₂O under D₂ gas the methane should be all CH₄; in other words $q = 1$ when $n_0 = 1$ and $q = 0$ when $n_0 = 0$ regardless of the hydrogen gas composition. At intermediate n_0 , q will be less than n_0 , and a plot of q vs. n_0 will give a hyperbola (Figure 1, dotted line, and Appendix 3). For case 4 there is always some intracellular H⁺ being produced from H₂ by hydrogenase, so that $q < 1$ even at $n_0 = 1$, and a plot of q vs. n_0 will give a straight line intersecting the $n_0 = 1$ axis at $q < 1$ (Figure 1, solid line, and Appendix 4). Conversely, in 100% H₂O under D₂ gas, case 4 predicts that some deuterated methane will be produced, i.e., $q > 0$ when $n_0 = 0$.

³ For cases 1 and 2 there is no production of H⁺ by hydrogenase ($k_3 = 0$), so that $n_i = n_0$. Therefore, $\alpha_{\text{obsd}} = \alpha_2$ (Appendix 2); that is, the observed isotope effect would be the intrinsic effect and independent of n_0 .

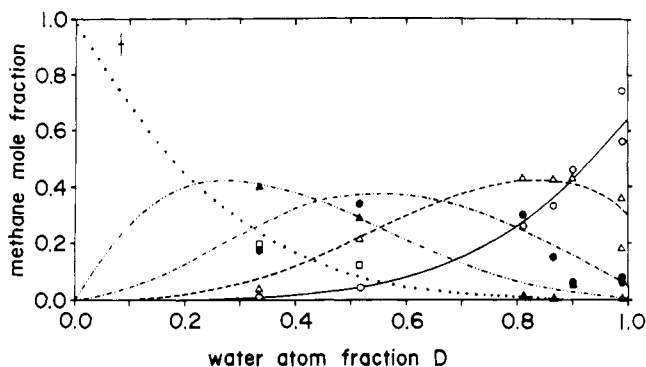


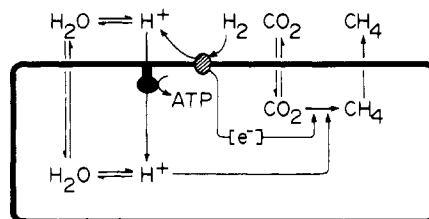
FIGURE 2: Distribution of deuterated methane species as a function of water deuterium enrichment. The symbols give the observed mole fractions of methane species (Table I) and the lines give the mole fractions predicted from case 4 (Appendices 1b and 4, with $\xi = 0.115$) as follows: CH_4 (\square and \cdots); CH_3D (\blacktriangle and \cdots); CH_3D_2 (\bullet and \cdots); CHD_3 (\triangle and \cdots); CD_4 (\circ and \cdots). The error bars for the experimental data are given in the upper left corner.

The experimental data (Table I) are plotted as q vs. n_0 in Figure 1. The simplest case in which there is neither isotope discrimination nor significant hydrogenase flux is given by the dashed line, $q = n_0$, and is excluded by the data. The distinction between cases 3 and 4 is difficult to make on the basis of curve fitting; the dotted line is the best fit to the data for the algebra of case 3, with $\alpha_2\gamma = 1.8$ (Appendix 3). The solid line is the best fit for the algebra of case 4, with $\xi = 0.12$ (Appendix 4). While the data do not exclude that both cases may apply (i.e., there is both a significant flux from hydrogenase and an intrinsic isotope effect), whether or not case 4 applies at all can be answered by examining the extremes of water enrichment under both H_2 and D_2 gases.

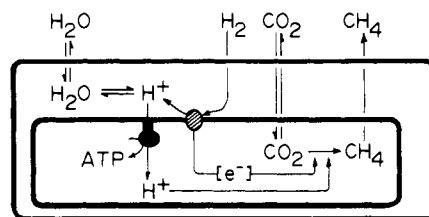
At the highest water enrichments achieved, the change from H_2 to D_2 gas effects an increase in the methane enrichment: from 98.7% D water under H_2 , the methane produced was 90% D (two separate experiments),⁴ while from 99.5% D water under D_2 the methane was 96% D. This suggests that most of the 10% H in the former experiment arose from H^+ produced from H_2 , i.e., that case 4 applies. More compelling is the result from 100% H_2O under D_2 gas; here the methane produced was 14% D. Since we have excluded direct transfer from hydrogen gas (Daniels et al., 1980), this deuterium in the methane must have arisen from intracellular D^+ produced by hydrogenase-catalyzed exchange from D_2 . These complementary experiments (86% H methane from 100% H_2O under D_2 and 90% D methane from 98.7% D_2O under H_2) are in close agreement.

The data also yield the intrinsic isotope effect α_2 from a plot of α_{obs} vs. $1/(1 - n_0)$ (Appendix 4; plot not shown). From such a plot, $\alpha_2 = 1.2 \pm 0.1$. Finally, with the relation between q and n_0 established (Appendix 4), the distribution of methane species can be predicted for all water enrichments (Appendix 1b). Figure 2 shows the excellent agreement between the predicted and observed methane distributions, verifying case 4 and, incidentally, confirming our earlier conclusion (Daniels et al., 1980) that all four of the hydrogens in methane have their origin in water and not hydrogen gas. It remains only

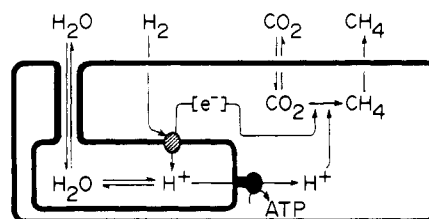
⁴ The two experiments at 98.7 atom % D water differ in the times of incubation which principally affects the hydrogen gas exchange (40 atom % D hydrogen gas at 2 h vs. >48 atom % D at 15 h). The methane enrichments are much less sensitive (87 and 92 atom % D), confirming the water origin of methane hydrogen. The difference in methane enrichment probably reflects decreased H^+ production by hydrogenase at long incubation times when a significant amount of the hydrogen gas has exchanged to HD and D_2 .



A



B



C

FIGURE 3: Hypothetical scheme for protonmotive force generation by hydrogenase and the methanogenic system. The hatched circles represent hydrogenase and the filled symbols represent ATPase. Reducing equivalents ($[e^-]$) are carried by redox coenzymes or electron transferring proteins. Not shown are any nucleotide translocases or potassium/proton antiporters (Doddema et al., 1979) that may also be involved.

to suggest interpretations for the magnitude of the intrinsic isotope effect α_2 , and the implications of this result in the production of a chemiosmotic proton gradient.

Extracts of *Methanobacterium bryantii* produce methane from H_2 and CO_2 but do not synthesize ATP from ADP and inorganic phosphate (Robertson & Wolfe, 1969), and intact, air-killed *M. thermoautotrophicum* produces ATP when pulsed with acid (Doddema et al., 1979). This suggests that methanogens may generate ATP at the expense of protons moving down a chemiosmotic gradient rather than by substrate-level phosphorylation. If this were the case, some of the energy of eq 1 (a total of 131 kJ/mol of CO_2) must be expended in proton transport at one or more steps. A plausible candidate for such a proton porter is a membrane-associated hydrogenase (Schneider & Schlegel, 1977); presumably the electron would reduce an intracellular acceptor (of sufficiently high potential to make proton transport favorable), and both protons from H_2 would be released outside the cell. Additional protonmotive force could be generated by the net consumption of protons in the reduction of CO_2 to methane (Figure 3A). This is not the case, since our results show that one or both protons from H_2 must be released intracellularly. This suggests that either (1) hydrogenase is not involved in the production of a proton gradient or (2) if it is involved, that gradient is established between the cytosol and vesicles seen in these bacteria (Zeikus & Wolfe, 1973; Doddema et al., 1979) (parts B and C of Figure 3). If these vesicles are closed, the fact that ATP is produced when air-killed whole cells are pulsed with acid (Doddema et al., 1978) suggests that the ATPase

Table II: Water Diffusion Exchange Times

system	exchange times		obsd/ free diffusion
	free diffusion ^a (μ s)	obsd (ms)	
erythrocytes	160	8-10 ^b	50
lecithin vesicles	0.005	0.4 ^c	9×10^4
<i>M. thermoautotrophicum</i>	2	2 ^d	10 ⁶

^a The exchange time for the same volume and shape in the absence of any membrane (Appendix 6). ^b At 37 °C (Conlon & Outhred, 1972). ^c At 37 °C (Andrasko & Forsen, 1974). ^d At 65 °C (our data). This value is in units of seconds.

and hydrogenase are oriented as in Figure 3B; this is also consistent with the enzyme staining results of Doddema et al. (1979). Protonmotive force production without postulating additional proton porters requires that the CO₂ reduction enzymes be intravesicular as shown. If the vesicles are continuous with the outside medium (Zeikus & Wolfe, 1973; Doddema et al., 1979), the acid pulsing results suggest the orientation of Figure 3C. Carbon dioxide reduction could again supply additional protonmotive force if located in the cytosol as shown.

The ratio of proton flux from H₂ and hydrogenase to that from extracellular water by diffusion [$=k_3/k_1([H_0^+] + [D_0^+])$] is 0.12, as determined from the right vertical intercept of Figure 1 (Appendix 4). Since the H⁺ production rate of hydrogenases can be estimated from in vivo measurement of both methanogenesis and the H₂ → HD and D₂ exchange reactions (Daniels et al., 1980), it is possible to estimate the rate of water diffusion through the membrane of the cells and compare it to water diffusion rates in other systems.

From the stoichiometry of methanogenesis (eq 1), up to eight intracellular H⁺ should be produced by hydrogenase per methane, depending on the proportion of H⁺ released inside the cell. Hydrogenases also catalyze hydrogen gas/water exchange (e.g., H₂ + D₂O → HD + HOD) that may be much more rapid than net turnover (Krasna & Rittenberg, 195; Yagi et al., 1973). We estimate that this exchange may exceed the rate of methane formation by a factor of 170 in vivo [Figure 1 in Daniels et al. (1980)]. As many as 40 H⁺ may be produced intracellularly per H⁺ removed as CH₄, so that $k_2 \ll k_3$ in Scheme 1.⁵ Note that this is production of label, i.e., H⁺ in D₂O, principally by the exchange reaction; the cells neither acidify nor alkalinize their medium, in agreement with the stoichiometry of eq 1. From this ratio (k_2/k_3), the known production of methane per milligram of cell protein, and estimates of cell volume and protein content, the time required for hydrogenase to produce 1/e the amount of total intracellular H⁺ is ~20 s (Appendix 5). Since experimentally this flux is 0.12 that of diffusion (Figure 1), the diffusion exchange time should be ~2 s. Water diffusion exchange times have been measured in erythrocytes and lecithin vesicles by ³H₂O label exchange and NMR relaxation techniques (Maloney et al., 1975); typical exchange times for these systems range from 0.4 to 9 ms at 37 °C and may be short as 70 μ s when extrapolated to 65 °C (Andrasko & Forsen, 1974). These exchange times can be properly compared in reference to calculated free diffusion exchange times for the same geometries

(Appendix 6). As seen in Table II, erythrocytes are quite permeable to water, retarding exchange by only a factor of 50, while lecithin vesicles retard exchange by a factor of nearly 10⁵. From our estimated exchange time for *M. thermoautotrophicum*, we calculate that these cells are even less permeant to water, retarding exchange by a factor of ~10⁶. Two possible contributions to this low water permeability can be suggested: first, the methanogens' membranes are composed of squalenes and isopranyl ethers (Tornabene & Langworthy, 1979; Tornabene et al., 1978) which may be inherently less permeant than fatty acyl ester membranes. The proton impermeability of *Thermoplasma acidophilum*, an acidophilic archaeobacterium with similar lipids, has been noted by Searcy (1976). Second, these bacteria have numerous "triplet membrane" internal vesicles whose total surrounding membranes are typically 260 Å thick (Zeikus & Wolfe, 1973). If methane and H⁺ from H₂ are produced within these structures, it is possible that equilibration with extracellular water (through the triplet membrane, plasma membrane, and cell wall) is indeed as slow as we have estimated.

The intrinsic deuterium product isotope effect in methanogenesis, α_2 , is 1.2 ± 0.1 . This is the range expected for equilibrium isotope effects (Schowen, 1977) and encompasses the effects for fixation of natural abundance deuterium from water into cellular material by plants and photosynthetic and methanogenic bacteria (Ziegler et al., 1976; Quandt et al., 1977; Fuchs et al., 1979). It would be of interest to determine this number at the precision possible in natural abundance measurements, since *M. thermoautotrophicum* shows an unusually large selection against ¹³CO₂ in methanogenesis [$\Delta\delta$ (¹³C) = -34% (Fuchs et al., 1979)] and Ziegler et al. (1976) have demonstrated a distinct correlation between ¹³C and ²H discriminations in CAM plants.

A basic question in the metabolism of methanogens is whether or not anabolic and catabolic CO₂ reduction pathways share any common intermediates. The ¹³C discrimination data of Fuchs et al. (1979) suggest that they do not, and the intrinsic deuterium discrimination in methanogenesis is small and sufficiently close to the discrimination against deuterium in production of cellular material [1.17 (Fuchs et al., 1979)] to suggest that the question may not be resolved by such whole cell isotope discrimination experiments. The methanogenic pathway has also been explored in classical labeling experiments (Daniels & Zeikus, 1978) and by partial purification of some of its component enzymes and coenzymes (Taylor & Wolfe, 1974; Romesser, 1978). Though the ultimate origin of hydrogen in methane is water and the hydrogen is incorporated with negligible isotope discrimination, in vitro studies with extracts and purified enzymes may reveal significant kinetic isotope effects from such possible proximal hydrogen donors as NADPH or dihydroF₄₂₀. For example, suppose F₄₂₀ on reduction acquires H or D from water with only an equilibrium isotope effect. In a subsequent reaction that dihydroF₄₂₀ may reduce a methane precursor CH₂=X to CH₃-XH or CH₂D-XH with a high V_{\max} isotope effect. However, if this enzyme has a high commitment to catalysis, the product isotope effect (which is a V/K effect) may be very low (Northrop, 1975), masking all but the original equilibrium effect.

Finally, with reference to Figure 3, it should be emphasized that our data requiring that the protons arising from the action of hydrogenase be produced *inside* the cell, along with a chemiosmotic hypothesis (in which a protonmotive force is produced during methanogenesis (eq 1) which then drives ATP synthesis), require that the separation of electrons and protons

⁵ This is independent evidence that it is case 4 rather than case 3 that applies. In case 3 (Appendix 3) the maximum possible α_1 is 2^{1/2} and could only be seen if the proton sink (k_2) is large compared to diffusion (k_1). The low rate of methane production compared to estimated diffusion rates suggests the opposite, i.e., that $\gamma = 1$ and that α_1 cannot account for the high values of α_{obsd} (all > 2^{1/2}).

takes place between compartments within the cell excluding the mechanism of Figure 3A. As can be appreciated from parts B and C of Figure 3, a decision between the two kinds of mechanisms may be possible if the locale of methanogenesis (intra- or extravesicular) can be ascertained and if acid- or base-driven ATP production can be demonstrated with suitable vesicle preparations.

Acknowledgments

We thank Gregory Kaczorowski, David Nelson, Harry Peck, and Alan Rendina for helpful discussions, J. G. Zeikus for cultures of the bacteria, and Mel Micke for expert assistance with the mass spectrometry.

Appendix

1. *Methane Distributions.* (a) *General Case.* Four hydrogens are acquired by the methanogenic carbon; let p_i and q_i be the probabilities that the i th hydrogen is protium or deuterium, respectively. The mole fractions of the five methane species are then

$$X_{CH_4} = p_1 p_2 p_3 p_4$$

$$X_{CH_3D} = \sum (p_h p_i p_j q_k) \text{ (four terms)}$$

$$(h, i, j, \text{ and } k = 1, 2, 3, \text{ and } 4)$$

$$X_{CH_2D_2} = \sum (p_h p_i q_j q_k) \text{ (six terms)}$$

$$X_{CHD_3} = \sum (p_h q_i q_j q_k) \text{ (four terms)}$$

$$X_{CD_4} = q_1 q_2 q_3 q_4$$

Each p_i and q_i is a function both of the water enrichment (n_0) and any isotope effect in the i th hydrogen transfer.

(b) *Specific Case.* If all steps have the same isotope effect, $p_1 = p_2 = p_3 = p_4$ and $q_1 = q_2 = q_3 = q_4$. The methane distribution then simplifies to the expansion of $(p + q)^4$ or

$$X_{CH_4} = p^4$$

$$X_{CH_3D} = 4p^3q$$

$$X_{CH_2D_2} = 6p^2q^2$$

$$X_{CHD_3} = 4pq^3$$

$$X_{CD_4} = q^4$$

2. *Calculations.* For a simple reaction involving acquisition of a proton or deuteron from water, the probability p that H^+ is acquired is proportional to $^Hk[H^+]$, where Hk is the rate of the reaction in 100% H_2O . Similarly, the probability q that D^+ is acquired is proportional to $^Dk[D^+]$. Letting $\alpha = ^Hk/^Dk$ and n = atom fraction of D of water = $[D^+]/([H^+] + [D^+])$ and normalizing such that $p + q = 1$

$$p = \frac{\alpha}{\alpha + n/(1-n)} \quad q = 1 - p = \frac{1}{\alpha(1/n - 1)}$$

and solving for α

$$\alpha = (1/q - 1)/(1/n - 1)$$

In our experiments the observed data are the mole fractions of methane species ($X_{CH_4D_{4-n}}$) and enrichment of bulk water (n_0). From the $X_{CH_4D_{4-n}}$ is calculated the atom fraction of D of the total methane, q :

$$q = (X_{CH_3D} + 2X_{CH_2D_2} + 3X_{CHD_3} + 4X_{CD_4})/4$$

This q is identical with that used in Appendix 1b.

The apparent product isotope effect α_{obsd} is calculated by using the bulk water enrichment $n_0 = [D_0^+]/([H_0^+] + [D_0^+])$ (see Scheme I)

$$\alpha_{\text{obsd}} = (1/q - 1)/(1/n_0 - 1) \quad (A1)$$

and the intrinsic product isotope effect α_2 is defined in terms of the intracellular² water enrichment $n_i = [D^+_i]/([H^+_i] + [D^+_i])$ as

$$\alpha_2 = (1/q - 1)/(1/n_i - 1) \quad (A2)$$

The relations between α_{obsd} and α_2 and n_i and n_0 are examined in Appendices 3 and 4.

3. *Calculations for Case 3.* All rate constants and concentrations refer to Scheme I. If the apparent isotope effect is due to discriminations in diffusion (k_1 's) and methanogenesis (k_2 's) and not H^+ from hydrogenase, i.e., $k_3 = 0$; α_1 and α_2 can be defined as $\alpha_1 = ^Hk_1/^Dk_1$ and $\alpha_2 = ^Hk_2/^Dk_2$ and n_i and n_0 are defined as in Appendix 2. At the steady state, $d[H^+_i]/dt = 0$ and $d[D^+_i]/dt = 0$, therefore

$$[H^+_i] = [H^+_0] \frac{^Hk_1}{^Hk_{-1} + ^Hk_2}$$

and

$$[D^+_i] = [D^+_0] \frac{^Dk_1}{^Dk_{-1} + ^Dk_2}$$

Since the k_1 's and k_{-1} 's are diffusion rates, $^Hk_1 = ^Hk_{-1}$ and $^Dk_1 = ^Dk_{-1}$, so that

$$n_i = n_0/[n_0 + \gamma(1 - n_0)]$$

where

$$\gamma = \text{constant} = \frac{1 + ^Hk_2\alpha_1/^Hk_1\alpha_2}{1 + ^Hk_2/^Hk_1}$$

This is the relation required to relate q and n_0 ; from eq A1 and A2 (Appendix 2)

$$q = [\alpha_2\gamma(1/n_0 - 1) + 1]^{-1}$$

For $\alpha_2\gamma > 1$, this yields hyperbolas in plots of q vs. n_0 , with intercepts at (0, 0) and (1, 1) (Figure 1, dotted line).

4. *Calculations for Case 4.* If the apparent isotope effect is due to H^+ from H_2 produced intracellularly, i.e., $k_3 > 0$, with α_1 , α_2 , n_i , and n_0 defined as before, at the steady state

$$[H^+_i] = \frac{[H^+_0]^Hk_1 + k_3}{^Hk_{-1} + ^Hk_2}$$

and

$$[D^+_i] = [D^+_0] \frac{^Dk_1}{^Dk_{-1} + ^Dk_2}$$

Using eq A1 and A2 (Appendix 2) and solving for q

$$q = [[\alpha_2(1 - n_0 + \xi)/n_0] + 1]^{-1}$$

where

$$\xi = \text{constant} = k_3\alpha_2/[k_1([H^+_0] + [D^+_0])]$$

If there is no intrinsic isotope effect, i.e., $\alpha_2 = 1$, this simplifies to

$$q = n_0/(\xi + 1)$$

which in plots of q vs. n_0 is a straight line intersecting at (0, 0) and $[1, 1/(\xi + 1)]$ (Figure 1, solid line).

In addition, these relations when solved for α_{obsd} give

$$\alpha_{\text{obsd}} = \alpha_2 + \xi/(1 - n_0)$$

so that a plot of α_{obsd} vs. $1/(1 - n_0)$ is linear with intercept α_2 and slope ξ .

5. *Estimating the in Vivo Water Exchange Time.* *M. thermoautotrophicum* are rods of $\sim 0.5\text{-}\mu\text{m}$ diameter and $3\text{-}\mu\text{m}$ length (Zeikus & Wolfe, 1973), implying an internal volume of $6 \times 10^{-10} \mu\text{L}$ and water proton content of $4 \times 10^{10} \text{H}^+$. Assuming $2 \mu\text{L}$ of internal volume/mg dry weight (Maloney et al., 1975) and 40% protein by dry weight, the typical methane production of the cells ($0.07 \mu\text{mol}$ of $\text{CH}_4 \text{ s}^{-1}$ mg of protein $^{-1}$) can be expressed as 4.8×10^6 molecules $\text{CH}_4 \text{ s}^{-1} \text{ cell}^{-1}$. Since H^+ production from H_2 can exceed CH_4 production by 170-fold (Daniels et al., 1980), intracellular H^+ production may be $8 \times 10^8 \text{H}^+ \text{ s}^{-1} \text{ cell}^{-1}$. This implies that the time required for hydrogenase to produce $1/e$ the number of intracellular protons is $\sim 20 \text{ s}$.

6. *Free Diffusion Solutions for Different Geometries.* Solution of the diffusion equation, $\partial c/\partial t = D\nabla^2 c$, are presented by Kotyk & Janáček (1975) for plane sheet, spherical, and cylindrical surfaces. The first term of each series has been solved for the exchange time τ (the time required for the internal label to decrease to $1/e$ of its initial value; $\tau = t_{1/2}/\ln 2$) with the following results

plane sheet of thickness d : $\tau = 0.55d^2/D$

sphere of radius r : $\tau = 0.029r^2/D$

cylinder of radius r : $\tau = 0.081r^2/D$

where $D = 2.5 \times 10^{-5} \text{ cm}^2/\text{s}$ for water.

Erythrocyte free exchange is approximated by that of a plane sheet half the thickness of an erythrocyte ($1.7 \mu\text{m}$), vesicle free exchange is approximated by that of a sphere of radius $0.02 \mu\text{m}$ (Andrasko & Forsén, 1974), and *M. thermoautotrophicum* free exchange is approximated by a cylinder of radius $0.25 \mu\text{m}$ (Zeikus & Wolfe, 1973) to give the values in Table II.

References

- Andrasko, J., & Forsén, S. (1974) *Biochem. Biophys. Res. Commun.* **60**, 813–819.
- Conlon, T., & Outhred, R. (1972) *Biochim. Biophys. Acta* **288**, 354–361.
- Daniels, L., & Zeikus, J. (1978) *J. Bacteriol.* **136**, 75–84.
- Daniels, L., Fulton, G., Spencer, R., & Orme-Johnson, W. (1980) *J. Bacteriol.* **141**, 694–698.
- Doddema, H., Hutten, T., van der Drift, C., & Vogels, G. (1978) *J. Bacteriol.* **136**, 19–23.
- Doddema, H., van der Drift, C., Vogels, G., & Veenhuis, M. (1979) *J. Bacteriol.* **140**, 1081–1089.
- Eirich, L., Vogels, G., & Wolfe, R. (1978) *Biochemistry* **17**, 4583–4593.
- Fuchs, G., Thauer, R., Ziegler, H., & Stichler, W. (1979) *Arch. Microbiol.* **120**, 135–139.
- Kotyk, A., & Janáček, K. (1975) *Cell Membrane Transport: Principles and Techniques*, 2nd ed., pp 38–39, Plenum Press, New York.
- Krasna, A., & Rittenberg, D. (1954) *J. Am. Chem. Soc.* **76**, 3015–3020.
- Maloney, P., Kashnet, E., & Wilson, T. (1975) *Methods Membr. Biol.* **5**, 2–4.
- Northrop, D. (1975) *Biochemistry* **14**, 2644–2651.
- Quandt, L., Gottschalk, G., Ziegler, H., & Stichler, W. (1977) *FEMS Microbiol. Lett.* **1**, 125–128.
- Robertson, A., & Wolfe, R. (1969) *Biochim. Biophys. Acta* **192**, 420–429.
- Romesser, J. (1978) Ph.D. Dissertation, University of Illinois at Urbana-Champaign.
- Schneider, K., & Schlegel, H. (1977) *Arch. Microbiol.* **122**, 229–238.
- Schowen, R. (1977) in *Isotope Effects on Enzyme-Catalyzed Reactions* (Cleland, W., O'Leary, M., & Northrop, D., Eds.) pp 64–99, University Park Press, Baltimore, MD.
- Searcy, D. (1976) *Biochim. Biophys. Acta* **451**, 278–286.
- Taylor, C., & Wolfe, R. (1974) *J. Biol. Chem.* **249**, 4879–4885.
- Tornabene, T., & Langworthy, T. (1979) *Science (Washington, D.C.)* **203**, 51–53.
- Tornabene, T., Wolfe, R., Balch, W., Holzer, G., Fox, G., & Oro, J. (1978) *J. Mol. Evol.* **11**, 259–266.
- Yagi, T., Tsuda, M., & Inokuchi, H. (1973) *J. Biochem. (Tokyo)* **73**, 1069–1081.
- Zeikus, J., & Bowen, V. (1975) *Can. J. Microbiol.* **21**, 121–129.
- Zeikus, J., & Wolfe, R. (1973) *J. Bacteriol.* **113**, 461–467.
- Ziegler, H., Osmond, C., Stichler, W., & Trimborn, P. (1976) *Planta* **128**, 85–92.